Analysis of Airborne Infrared Imagery from CBLAST-Low

Christopher J. Zappa
Lamont-Doherty Earth Observatory of Columbia University
Ocean and Climate Physics Division
61 Route 9W - PO Box 1000
Palisades, NY 10964
Phone: (845) 365-8547 fax: (845) 365-8157 email: zappa@ldeo.columbia.edu

Award Number: N00014-05-1-0036

Andrew T. Jessup
University of Washington
Applied Physics Laboratory
1013 NE 40th Street
Seattle, WA 98105-6698
Phone: (206) 685-2609 fax: (206) 543-6785 email: jessup@apl.washington.edu

Award Number: N00014-01-1-0080

LONG-TERM GOALS

The long-term goal is to understand the mechanisms that produce spatial variability in ocean surface skin temperature over a wide range of scales under low wind conditions.

OBJECTIVES

The first objective is to use an airborne infrared imager to produce both overview maps and high-resolution time series of thermal variability over the CBLAST study area. The second objective is to combine these data with measurements by other investigators to determine the extent to which horizontal variability in surface temperature is related to atmospheric and sub-surface phenomena.

APPROACH

The approach is to make airborne measurements of horizontal variability of ocean surface skin temperature during the CBLAST-LOW experiments using two complementary infrared (IR) sensors. An IR imaging system provided high spatial and temporal resolution while a narrow field-of-view (FOV) radiometer system provided calibrated surface temperature. The high spatial coverage and fine spatial and temperature resolution of our systems allowed us to examine spatial scales in skin temperature from processes that span the atmospheric boundary layer of O(1 km) down to wave-related processes O(1 m). We produce synoptic maps of temperature covering the CBLAST-LOW region at moderate altitude as well as observations of fine-scale structures. Flight tracks allowed us to utilize the offshore tower (instrumented by J. Edson – WHOI [*Edson, et al.*, 2004]) and horizontal ocean buoy array (deployed by R. Weller – WHOI [*Farrar, et al.*, 2004]) data sets as well as directly compare sea-surface signatures with the oceanic and atmospheric boundary layer processes and fluxes. For the 2nd experiment in August/September of 2002 and the 3rd field campaign in July/August of 2003, we made measurements of the sea surface and the sky with down- and up-looking AIM model

Report Documentation Page

Form Approved
OMB No. 0704-0188

1. REPORT DATE	2. REPORT TYPE	3. DATES COVERED
30 SEP 2005		**00-00-2005 to 00-00-2005**

4. TITLE AND SUBTITLE	5a. CONTRACT NUMBER
Analysis of Airborne Infrared Imagery from CBLAST-Low	5b. GRANT NUMBER
	5c. PROGRAM ELEMENT NUMBER
6. AUTHOR(S)	5d. PROJECT NUMBER
	5e. TASK NUMBER
	5f. WORK UNIT NUMBER
7. PERFORMING ORGANIZATION NAME(S) AND ADDRESS(ES)	8. PERFORMING ORGANIZATION REPORT NUMBER
Lamont-Doherty Earth Observatory of Columbia University,Ocean and Climate Physics Division,61 Route 9W - PO Box 1000,Palisades,NY,10964	
9. SPONSORING/MONITORING AGENCY NAME(S) AND ADDRESS(ES)	10. SPONSOR/MONITOR'S ACRONYM(S)
	11. SPONSOR/MONITOR'S REPORT NUMBER(S)

12. DISTRIBUTION/AVAILABILITY STATEMENT
Approved for public release; distribution unlimited

13. SUPPLEMENTARY NOTES
code 1 only

14. ABSTRACT
The first objective is to use an airborne infrared imager to produce both overview maps and high-resolution time series of thermal variability over the CBLAST study area. The second objective is to combine these data with measurements by other investigators to determine the extent to which horizontal variability in surface temperature is related to atmospheric and sub-surface phenomena.

15. SUBJECT TERMS

16. SECURITY CLASSIFICATION OF:			17. LIMITATION OF ABSTRACT	18. NUMBER OF PAGES	19a. NAME OF RESPONSIBLE PERSON
a. REPORT	b. ABSTRACT	c. THIS PAGE			
unclassified	**unclassified**	**unclassified**	**Same as Report (SAR)**	**10**	

640Q longwave (8-12 μm) IR imagers (512 x 640 pixels) and Heimann KT-15 radiometers (8-14 μm). A Pulnix digital video camera was implemented to characterize the sea surface condition.

WORK COMPLETED

We completed analysis on data taken during the CBLAST pilot experiment that occurred in July/August of 2001. These results have been published in *Geoscience and Remote Sensing Letters* [*Zappa and Jessup*, 2005]. We analyzed data taken during the 2nd CBLAST experiment in August-September of 2002 and presented the results at the recent *AMS 16th Symposium on Boundary Layers and Turbulence* [*Zappa and Jessup*, 2004]. A description of the airborne IR imagery system is given on the CBLAST-Low website (http://www.whoi.edu/science/AOPE/dept/CBLAST/CBLAST%20IR%20Description.htm). We participated in the 3rd and final CBLAST-Low experiment in July-August of 2003. The surveys in 2002 and 2003 quantified the horizontal mesoscale variability in the domain around the CBLAST-LOW site near the offshore tower and the horizontal ocean mooring/buoy array throughout the region extending 40-50 km offshore. Temperature maps from 2003 can be found on the CBLAST-Low website (http://www.whoi.edu/science/AOPE/dept/CBLAST/low/aircraft.html). The data have been cataloged (http://www.ldeo.columbia.edu/~zappa/CBLAST) and we have surveyed them for important results. We have quantified the SST variability and are beginning to determine the causes of the enhanced SST variability under low winds and its effect on air-sea heat fluxes.

RESULTS

The data collected during the CBLAST-Low field program has allowed substantial progress toward understanding the robust SST structure that occurs under low wind speeds. Data quality met or exceeded expectations, and all initial data processing and quality control is complete. Results based on analyses of our data have been presented at the 2004 AGU Ocean Sciences Meeting, the 2004 AMS Boundary Layers and Turbulence Conference, and the 2003 International Geoscience and Remote Sensing Symposium.

The IR imagery shows high temperature variability on scales of $O(10\text{ m} - 1\text{ km})$. Maps of sea surface temperature produced using the low-noise, high-resolution data from the longwave IR imager suggest that diurnal warming and tidal advection/mixing control the regional scales of SST. Results from the two weeks of flights in 2002 show that clear skies, strong insolation and moderate wind speeds lead to high SST variability (2.1°C in 10 km). The variability in SST is shown to diminish with the increase in overcast conditions and high wind speed events (1.5°C in 10 km). Measurements from 2003 show similar results with horizontal gradients reaching 4.5 °C in 10 km. Repeated flights give us the capability to track the diurnal variability of ocean surface temperature and allow us to determine the extent to which ocean mixing, advection, or heat flux variability is driving this temperature variability.

Two areas of recent progress which we are pursuing further are: 1) improved characterization of the Stanton and Dalton numbers based on SST variability at low wind speeds, 2) improved understanding of the processes responsible for increased SST variability under low winds. Work to date in each of these areas of progress is addressed below.

Effect of SST variability and heat flux

We estimated the heat flux variability due to ocean skin temperature alone by implementing the TOGA COARE algorithm for the scalar fluxes [*Fairall, et al.*, 1996]. Results from the two weeks of flights

during both the summers of 2002 and 2003 demonstrate that the average variability of scalar heat fluxes was ±8.0 W m^{-2} 10km^{-1} for the sensible and ±53.6 W m^{-2} 10km^{-1} for the latent. The model input parameters (wind speed, water vapor mixing ratio, and potential air temperature) were found to be relatively uniform within the CBLAST-LOW study site. Therefore, these results suggest that the heat flux variability is dominated by ocean skin temperature. The spatial variability of heat flux is important to the model development of the heat transfer coefficients since the spatial variability of the region is integrated into direct covariance flux measurements [*Edson, et al.*, 1998]. The integrated area that effects the covariance fluxes, or the flux footprint, is typically of *O*(1-10 km) and is dependent on the development of the boundary layer height and wind speed. An obvious question then follows: is some of the scatter commonly seen in plots of transfer coefficients correlated with the SST variability in the flux footprint? Can this be reduced using, e.g., the area averaged value of the SST? Figure 1 shows representative transects of the SST variability within the flux footprint of the ASIT and the Stanton number summary for CBLAST-Low during 2003 from ASIT. The SST variability is of the order ±0.5°C and initial indications in collaboration with J. Edson are that much of the variability in the Stanton number under stable conditions can be explained by the SST variability within the flux footprint.

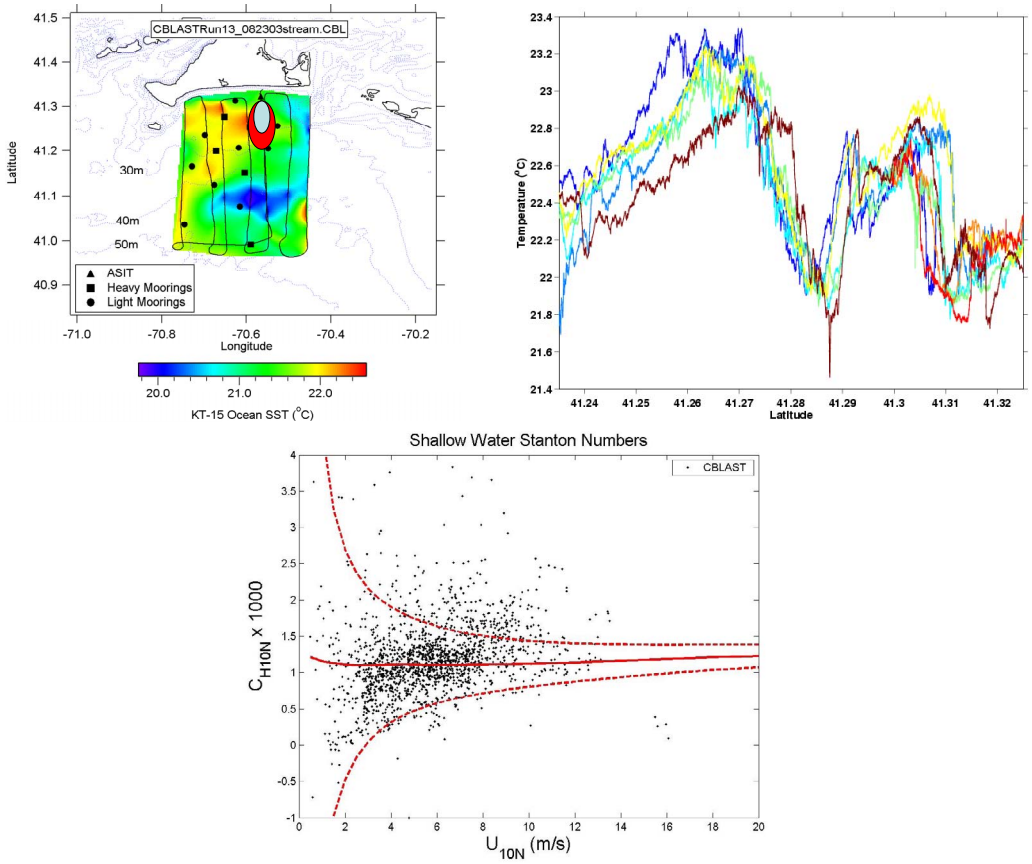

Figure 1. Top Left: Map of SST variability measured using the low-noise data from the imager (in Sub-Frame mode). The black trace is the Skymaster flight track, the triangle is the ASIT, the squares are the heavy moorings, and the circles are the light moorings. The ellipsoids are representative flux footprints in front of the ASIT for various wind speeds. Top Right: Transects of SST variability within the flux footprint. Bottom: Shallow-water Stanton numbers during CBLAST-Low 2003. Solid red line is the TOGA-COARE bulk formula version 3.0 and the dashed red traces are the error introduced when accounting for the SST variability within the flux footprint.

Effect of ocean processes on SST variability

The data taken during CBLAST-Low in 2002 and 2003 shows that the mean fine-scale variability decreases with wind speed. During these IOP experiments, we also observed remarkable variability in small-scale structures that suggests mechanisms related to subsurface phenomena that drive or enhance exchange. The 1-m resolution IR imagery shows high SST variability of several degrees on scales of *O*(10m – 1km) under a variety of wind speed conditions. The structure of this mean variability is evident in variance-preserving wavenumber spectra of the SST under conditions of very low wind to moderately high winds. Under low wind-speed conditions (0 to 2.5 m s^{-1}), the IR imagery shows high temperature variability on scales of *O*(1 m to 100 m) without the distinction of coherent structures. The spectra are characterized by a broad distribution of energy that decreases at high wavenumber with increasing wind speed. During one spectra at low wind, internal waves were present and a peak in the spectra occurred at a wavenumber of roughly 0.004 m^{-1}, that of the peak wavenumber for the internal waves. During moderate winds (2.5 to 5 m s^{-1}), the variability is on scales of *O*(100 m – 1 km) and is related to internal waves and coherent ramping structures. The spectra exhibit a significant energy drop at intermediate wavenumbers with a peak in wavenumber at roughly 0.01 m^{-1}, the scale of the coherent ramping structures. For wind speeds greater than 5 m s^{-1}, the data show significantly less temperature variability with incidence of breaking waves and distinct row/streak structures in the IR imagery that were aligned with the wind and were likely the surface manifestation of Langmuir circulation cells. Here, the energy in the spectra dips at intermediate wavenumbers but increase at higher wavenumber in the range 0.05 to 0.1 m^{-1}, the scales of observed Langmuir circulation. The wavenumber spectra in all wind-speed regimes are clearly affected and governed by the process within the near-surface ocean layer and/or the thermocline.

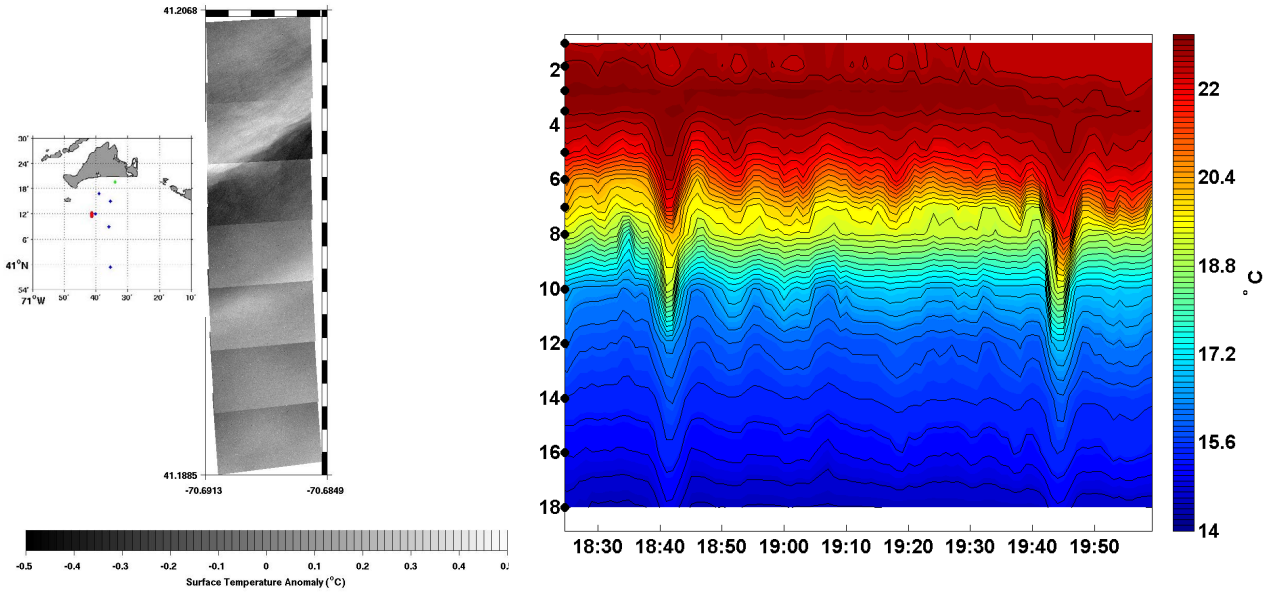

Figure 2. Mosaic (left) of SST anomaly over 2 km directly over a heavy mooring site at 1946 UTC. Time series of temperature field (right) at the mooring site shows the internal waves propagating onshore. Current vectors associated with 30-minute period internal waves were observed at two nearby heavy moorings during the hour centered on the aircraft overpass. The internal wave crests in the SST signature are oriented perpendicular to the axis of the internal wave velocity fluctuations observed at the moorings. The inset shows the CBLAST-Low region. The red dot is the location of the aircraft, the blue dots are the mooring sites, and the green dot is the location of ASIT.

A case study on Aug 14, 2003 of coincident airborne SST and oceanic mooring data provides a clear example of the internal wave signature imprinted in the SST variability. Figure 2 shows a mosaic of the SST anomaly over 2 km directly over a heavy mooring site at 1946 UTC. The leading edge in the SST mosaic shows an increase in temperature followed by an abrupt decrease and subsequent return to ambient SST that is coincident with the passage of the internal wave in the subsurface temperature data. The SST mosaic suggests internal waves propagating onshore with crests oriented 45° from North. Current vectors during the time of the aircraft overpass associated with 30-minute period quasi-linear, energetic internal waves were observed at two nearby heavy moorings. As would be expected, the horizontal velocity signal of the internal waves is rectilinear and perpendicular to the wave crest and trough signatures seen in the SST imagery.

Consistent with the observations of *Walsh et al.* [1998] and *Marmorino et al.* [2004], our analysis provides direct evidence that the SST spatial fluctuations are a surface expression of oceanic internal waves [*Farrar, et al.*, 2004]. However, it is still unclear how the subsurface temperature signal is imprinted on the sea surface. *Walsh et al.* [1998] hypothesized that the SST signal was caused by internal wave modulation of near surface mixing, while *Marmorino et al.* [2004] hypothesized that the SST signal was a result of vertical straining of the aqueous thermal boundary layer by the internal waves. Either mechanism may dominate for a given condition. Presently we are working closely with R. Weller and J. T. Farrar (WHOI) under the hypothesis that the surface signature is due to a combination of near surface mixing, which may directly imprint the signal on the surface, and the surface strain associated with the waves, which may modify the magnitude of the cool skin effect.

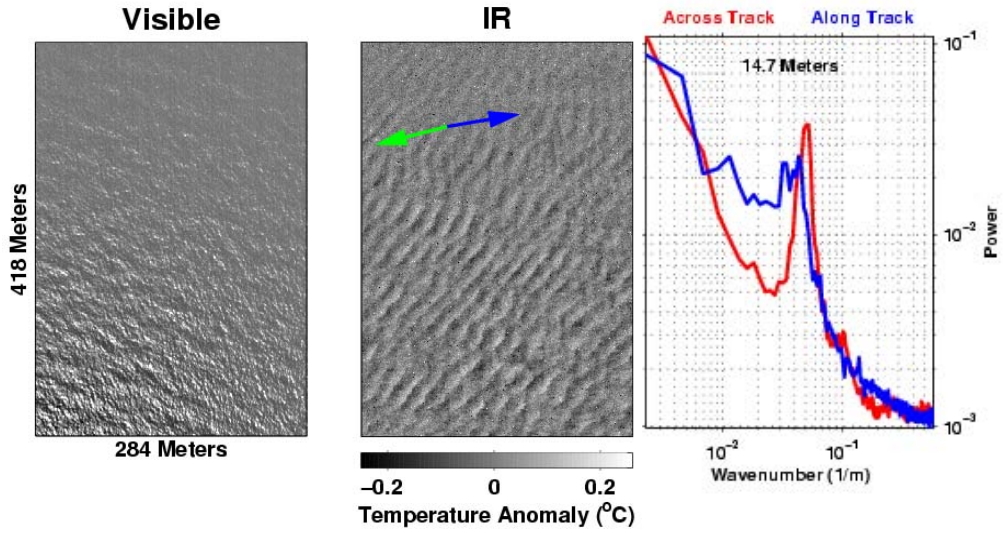

Figure 3. Video image, IR image, and spectra of the IR image showing coherent ramp structures observed on August 14, 2003 in the afternoon. The wind speed (Blue Arrow) is roughly 4 m s^{-1} from the West and the surface current (Green Arrow) is 17 cm s^{-1} from the East. The variability in temperature across these coherent ramps is of O(0.5 ºC), their dominant scale is 14.7 m, and they extend over several km. The lack of coherent parallel features in the video imagery suggests that the ocean surface features observed in the IR imagery are not related to surface gravity waves. Here, the skewness of the temperature variability is 2.8, strongly suggestive of "billows" from shear-induced turbulence.

We also observed extensive regions (O(1 km)) of successive sharp coherent temperature ramps of O(0.5ºC) with spacing of O(10 m) that coincide with visible surface slicks parallel to the fronts (see Figure 3) during moderate winds (2.5 to 5 m s^{-1}). These coherent ramp structures may be the IR signature of a mechanism in the near-surface layer that leads to the stratification breakdown under conditions when the turbulence transitions from a buoyancy- to a shear-driven state. The wind speed is roughly 4 m s^{-1} from the West and the surface current is 17 cm s^{-1} from the East. The dominant spatial scale of the variability in temperature across these coherent ramps is 14.7 m, and they extend over several km. The lack of coherent parallel features in the video imagery suggests that the ocean surface features observed in the IR imagery are not related to surface gravity waves. Here, the skewness of the temperature variability is 2.8, strongly suggestive of "billows" due to shear-induced instability.

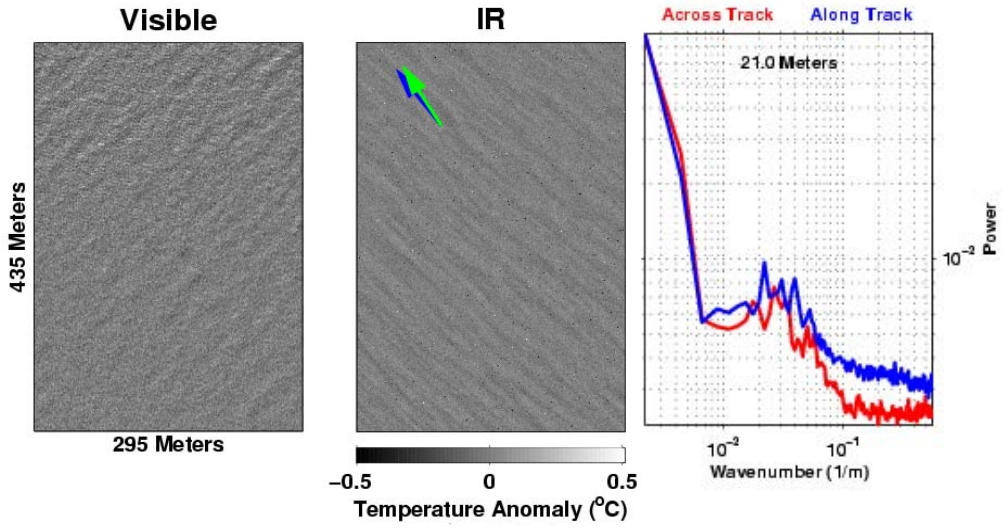

Figure 4. Video image, IR image, and spectra of the IR image depicting Langmuir circulation observed on August 25, 2003 in the morning. The wind speed (Blue Arrow) is roughly 5 m s^{-1} and the surface current (Green Arrow) is 47 cm s^{-1}, both from the West-SouthWest. The IR image shows an ocean surface with thin bands of cool water that are parallel to the wind and about 0.2°C less than the regions between the bands. The dominant scale between these cool bands is 21.0 m, the features are evident throughout the CBLAST-Low region, and the temperature variability is calculated to be Gaussian. These parallel-aligned structures with the wind and perpendicular to the waves in the video are suggestive of Langmuir circulation.

For wind speeds greater than 5 m s^{-1}, there is significantly less variability with distinct row/streak structures that were aligned with the wind and are likely due to Langmuir circulation cells (see Figure 4). The horizontal spacing of these features clearly increased from roughly 10 m up to 50 m with the increase in fetch offshore and coincided with wind-aligned surface slicks and bubbles visible in the video. The wind speed in Figure 4 is roughly 5 m s^{-1} and the surface current is 47 cm s^{-1}, both from the West-SouthWest. The IR image shows an ocean surface with thin bands of cool water that are parallel to the wind and about 0.2°C less than the regions between the bands. The dominant scale between these cool bands is 21.0 m, the features are evident throughout the CBLAST-Low region, and the temperature variability is calculated to be Gaussian. These parallel-aligned structures with the wind and perpendicular to the waves in the video are suggestive of Langmuir circulation. These fine-scale measurements demonstrate processes that directly affect the thermal boundary layer and therefore are important to upper-ocean mixing and transport dynamics as well as the magnitude and distribution of air-sea fluxes.

The distribution of length scales has been investigated by determining the dominant scale for individual IR images during CBLAST-Low 2003. Length scales are determined from individual images using an algorithm developed during this year that couples Radon Transform and FFT methodologies. Differences in the distributions are associated with different features. Figure 6 shows the distributions of length scales from three flights that were dominated by different features including coherent ramping structures (Top; as in Figure 3), coherent ramping structures within an active internal wave field (Middle), and Langmuir circulation (Bottom; as in Figure 4). The left graph in each is the distribution of length scales. Notice that the distribution of length scales for both the coherent ramping structures alone and Langmuir circulation are similarly weighted toward smaller scales less than 25 m. This is not surprising since the observed scales in Figures 3 and 4 are comparable. However, Langmuir circulation signatures are more prevalent. The comparable distributions for two distinct mechanisms suggest that another controlling factor such as depth may be important. However, the active internal wave field significantly modulates the coherent ramping structures causing the distribution to be weighted toward larger scales greater than 25 m as well as more instances of coherent structures. This suggests that the larger internal wave packets trigger smaller-scale disturbances within the near-surface layer.

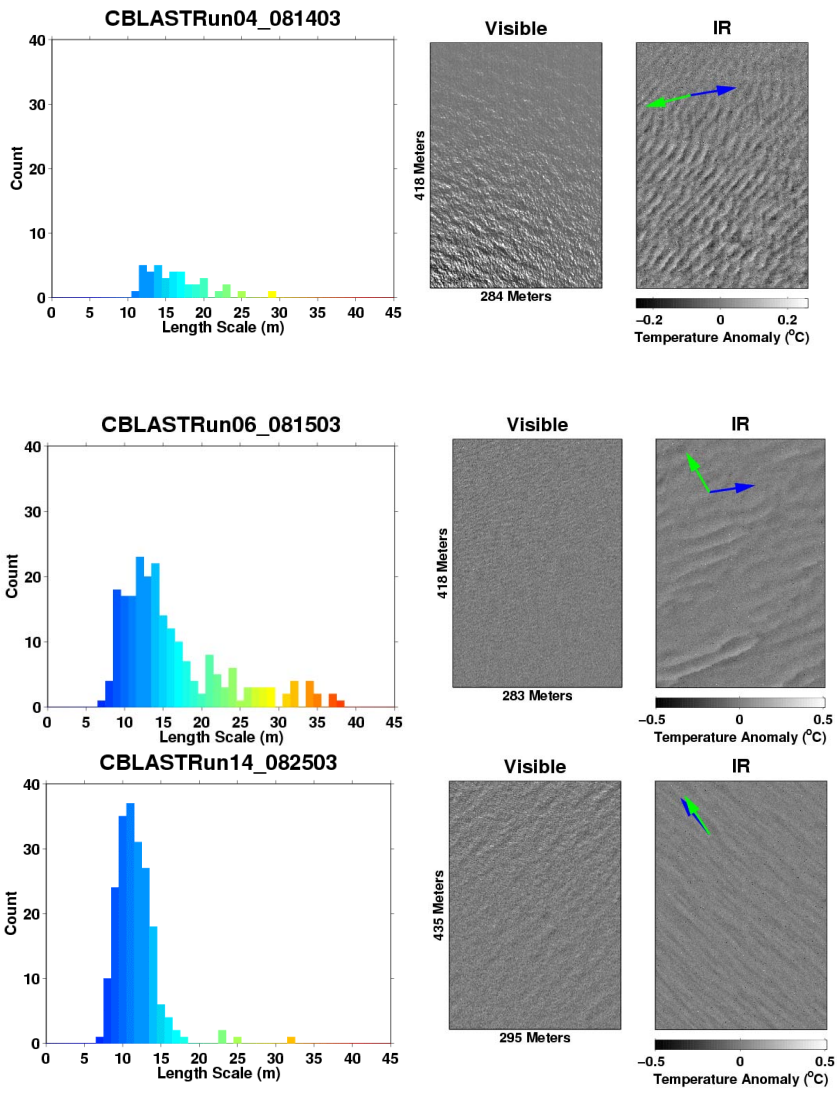

Figure 6. Distributions of length scales (Left plot in each pair) determined from individual IR images using the Radon processing method during CBLAST-Low 2003 for examples of coherent ramping structures (Top), coherent ramping structures within an active internal wave field (Middle) and Langmuir circulation (Bottom). On the right show the visible and IR imagery corresponding to the signature defining the distribution on the left.

IMPACT/APPLICATIONS

The encouraging results of our airborne deployments under the CBLAST DRI demonstrate that we are able to provide sea surface temperature measurements with high spatial resolution and accuracy. The impact of our analysis and observations will be to show that remote sensing techniques can quickly characterize the spatial and temporal scales of a wide variety of processes that are important to the air-sea fluxes, as well as to relate the fine-scale to the larger-scale variability. Processes related to mixing may both support and result from the horizontal inhomogeneities in the upper ocean. The IR measurements themselves have provided important two-dimensional structure of the ocean surface features that may be missed by *in-situ* measurements.

RELATIONSHIP TO OTHER PROGRAMS OR PROJECTS

We are working closely with R. Weller of WHOI to correlate the IR signatures with environmental conditions measured by the buoys deployed during CBLAST and at the ASIT tower.

REFERENCES

Edson, J. B., et al. (2004), Investigations of flux-profile relationships in the marine atmospheric surface layer during CBLAST, paper presented at 16th Symposium on Boundary Layers and Turbulence, Ref. 8.2, Portland, Maine, USA.

Edson, J. B., et al. (1998), Direct covariance flux estimates from mobile platforms at sea, *J. Atmos. Oceanic Tech*, *15*, 547 - 562.

Fairall, C. W., et al. (1996), Bulk parameterization of air-sea fluxes for Tropical Ocean Global Atmosphere Coupled Ocean Atmosphere Response Experiment, *Journal Of Geophysical Research*, *101*, 3747-3764.

Farrar, J. T., et al. (2004), Subsurface expressions of sea surface temperature variability under low winds, paper presented at 16th Symposium on Boundary Layers and Turbulence, Ref. P8.1, Portland, Maine, USA.

Marmorino, G. O., et al. (2004), Infrared imagery of ocean internal waves, *Geophys. Res. Lett.*, *31*, L11309, doi:11310.11029/12004GL020152.

Walsh, E. J., et al. (1998), Coupling of internal waves on the main thermocline to the diurnal surface layer and sea surface temperature during the Tropical Ocean-Global Atmosphere Coupled Ocean-Atmosphere Response Experiment, *Journal of Geophysical Research*, *103*, 12613-12628.

Zappa, C. J., and A. T. Jessup (2004), Variability of ocean skin temperature from airborne infrared imagery during CBLAST-Low, paper presented at 16th Symposium on Boundary Layers and Turbulence, Ref. 8.11, Portland, Maine, USA.

Zappa, C. J., and A. T. Jessup (2005), High resolution airborne infrared measurements of ocean skin temperature, *Geoscience and Remote Sensing Letters*, *2*, doi:10.1109/LGRS.2004.841629.

PUBLICATIONS

Zappa, C. J., and A. T. Jessup (2005), High resolution airborne infrared measurements of ocean skin temperature, *Geoscience and Remote Sensing Letters*, *2*, doi:10.1109/LGRS.2004.841629 [published, refereed].

Zappa, C.J., and A.T. Jessup, Variability of ocean skin temperature from airborne infrared imagery during CBLAST-Low, in *16th Symposium on Boundary Layers and Turbulence*, Ref. 8.11, Portland, Maine, USA, 2004 [published].